Article

Intestinal Microbial and Metabolite Profiling of Mice fed with Dietary Glucose and Fructose

João C.P. Silva[1], Marta Mota[1,2], Fátima O. Martins[1,3], Célia Nogueira[1,2], Teresa Gonçalves[1,2], Tatiana Carneiro[4], Joana Pinto[5], Daniela Duarte[4], Antonio S. Barros[6], John G. Jones[3,7†,*] and Ana M. Gil[3,†,*]

[1] CNC – Center for Neuroscience and Cell Biology, University of Coimbra, Portugal; john.griffith.jones@gmail.com
[2] Institute of Microbiology, Faculty of Medicine, University of Coimbra, Portugal
[3] CEDOC, NOVA Medical School, Universidade NOVA de Lisboa, Rua Camara Pestana, nº6, 6A, edifício II, piso 3, 1150-082 Lisbon, Portugal
[4] CICECO-Department of Chemistry, University of Aveiro, Campus de Santiago, 3810-193 Aveiro, Portugal; e-mail: agil@ua.pt
[5] UCIBIO@REQUIMTE/Toxicological Laboratory, Biological Science Department, Faculty of Pharmacy, Univeristy of Porto, 4050-313 Porto, Portugal
[6] Department of Cardiothoracic Surgery and Physiology, Faculty of Medicine, Porto 4200-319, Portugal
[7] APDP – Portuguese Diabetes Association, Lisbon, Portugal

† these authors contributed equally to this paper.
* Correspondence: john.griffith.jones@gmail.com; Tel.: +351231249181; agil@ua.pt, tel:+351234370707

Abstract: Increased sugar intake is implicated in Type-2 diabetes and fatty liver disease. Mechanisms by which glucose and fructose components promote these conditions are unclear. We hypothesize that alterations in intestinal metabolite and microbiota profiles specific to each monosaccharide are involved. Two groups of six adult C57BL/6 mice were fed for 10-weeks with a diet where either glucose or fructose was the sole carbohydrate component (G and F, respectively). A third group was fed with normal chow (N). Fecal metabolites were profiled every 2-weeks by ^{1}H NMR and microbial composition was analysed by real-time PCR (qPCR). Glucose tolerance was also periodically assessed. N, G and F mice had similar weight gains and glucose tolerance. Multivariate analysis of NMR profiles indicated that F mice were separated from both N and G, with decreased butyrate and glutamate and increased fructose, succinate, taurine, tyrosine and xylose. Compared to N and G, F mice showed a shift in microbe populations from gram-positive *Lactobacillus spp.* to gram-negative *Enterobacteria* species. Substitution of normal chow carbohydrate mixture by either pure glucose or fructose for 10 weeks did not alter adiposity or glucose tolerance. However, F G and N mice generated distinctive fecal metabolite signatures with incomplete fructose absorption as a dominant feature of F mice.

Keywords: Fructose; intestinal microbiota; short-chain fatty acids; metabolic profiling

1. Introduction

In recent decades, Western societies have seen steep increases in obesity rates and a surge of associated complications such as non-alcoholic fatty liver disease (NAFLD) and Type 2 Diabetes (T2D) [1-3]. Over this same period, the average daily caloric intake has risen, driven in large part by a substantial increase in sugar consumption [4]. In European countries, sugar is consumed as sucrose, while in North America there has been an increased utilization of high fructose corn syrup (HFCS). Both formulations result in the delivery of approximately equivalent amounts of glucose and fructose to the gastrointestinal tract (sucrose being rapidly hydrolysed to fructose and glucose in the upper small intestine) followed by absorption of glucose and fructose by specific transporters:

 doi:10.20944/preprints201801.0210.v1

SGLT1 for glucose and GLUT5 and GLUT2 for fructose. Therefore, when sugar intake is low, these monosaccharides are rapidly and quantitatively absorbed becoming unavailable for intestinal microbiota metabolism – particularly those residing in the lower intestine. However, with high sugar intake, these transporters – particularly those involved with fructose uptake - may become saturated thereby increasing the residence time of monosaccharides in the intestinal lumen and providing an increased opportunity for metabolism by the intestinal microbiota.

There is now extensive evidence that interactions between the gut microbiota and diet promote obesity *per se* as well as obesity-related complications such as NAFLD and T2D [5]. In animal models, high fat feeding resulted in impaired intestinal integrity and leakage of pro-inflammatory endotoxins into the portal vein blood that in turn provoked hepatic inflammation. This process was associated with a shift in intestinal bacterial species distribution [6,7]. Diet composition has also been shown to alter intestinal metabolite, including those generated by microbial activity such as short-chain fatty acids. These changes can be noninvasively followed by metabonomic analysis of feces [8-10].

Of the monosaccharide components of dietary sucrose or high-fructose corn syrup (HFCS), fructose is more pro-inflammatory and lipogenic to liver than glucose [11-14]. To date, the search for possible mechanisms has focused on liver, since this organ is responsible for the majority of systemic fructose metabolism. We hypothesized that, in addition to hepatic mechanisms, part of the deleterious effects of high fructose feeding are mediated through specific interactions of fructose with intestinal microbiota. To untangle the possible effects of fructose from those of glucose, which are consumed in approximately equivalent amounts even in the so-called "high fructose diets", we compared *Lactobacillus* and *Enterobacteria*, representative of gram positive and gram negative bacterial populations of the intestinal microbiota and metabolite profiles of mice fed with diets whose carbohydrate components were solely comprised of fructose or glucose. To determine the effects of replacing the standard dietary mixture of simple and complex carbohydrates by either of these simple sugars on intestinal microbota and metabolite profiles, a third group of animals fed on normal chow was also included in the study. Aiming to target the specific effect of simple sugars this experimental design was a missing approach on the clean and direct effects of dietary glucose and fructose in the correlation of gut metabolism and microflora.

2. Materials and Methods

2.1 Animal model

All animal studies were approved by the University of Coimbra Ethics Committee on Animal Studie ORBEA (responsible body for the animal wellbeing) and the Portuguese National Authority for Animal Health (DGAV), approval code 0421/000/000/2013. Eighteen adult male C57BL/6 mice were obtained from Charles River Labs, Barcelona, Spain, and housed at the University of Coimbra Faculty of Medicine Bioterium. They were maintained in a well-ventilated environment, in 12 h light/12h dark cycle (lights on from 7:00.19:00) according a protocol approved by the local Ethics Committee. Upon delivery, mice were provided two weeks to adjust to their Bioterium housing with free access to food (standard chow – 60% carbohydrate, 16% protein and 3% lipid) and water. After this period animals were randomly assigned to three synthetic diets supplied by Special Diets Services, Argenteuil, France over a 10-week period. These were standard chow (60% carbohydrate, 16% protein and 3% lipid by weight); high glucose (60% glucose, 16% protein and 3% lipid by weight); high fructose (60% fructose, 16% protein and 3% lipid by weight). These synthetic diets were formulated on an AIN-93G background and packaged in coarse powder form (the high glucose and fructose formulations could not be pelletized). For this reason, the mice were provided with the powdered standard chow placed in small open Petri dishes during the initial 2-week adjustment period and this method of feed delivery was used in the subsequent studies. Hereafter, the three diets will be referred to as normal-chow, glucose-chow, and fructose-chow.

 doi:10.20944/preprints201801.0210.v1

2.2 Sample Collection:

Fecal samples were collected every two weeks for analysis by ^{1}H NMR spectroscopy and qPCR. Collections were performed on three consecutive days, one day for each different diet, and six mice at a time in a clean and sterile flow chamber to minimize sample contamination. One-half of each feces sample was used for NMR studies and the other half for qPCR analysis. Feces samples were immediately stored in Eppendorf tubes and immediately frozen in liquid nitrogen followed by storage at -80 °C until further processing and analysis.

2.3 Oral glucose tolerance test

Mice were fasted throughout the overnight dark period and through the initial 4 h of the light period for a total time of 16 h. Mice were then gavaged with a solution of 10% glucose prepared in sterilized drinking water whose volume corresponded to 2 mg glucose/ g body weight. Blood glucose levels were monitored from tail tip samples at 0, 15, 30, 60 and 120 min after gavage using a OneTouch Vita (LifeScan) glucometer.

2.4 Metabolite extraction:

Processing of samples to obtain fecal extracts was performed according to previously published methods [15,16]. Briefly, 70 mg of thawed stool samples were homogenized by vortex mixing in 700 µl phosphate buffer (0,1M K_2HPO_4/NaH_2PO_4, pH 7.4) containing 10% D_2O, 0.01% (w/v) of NaN_3 and 0.5 mM of sodium 3-([2,2,3-d_4]trimethylsilyl) propionate (TSP). After mixing, samples were submitted to 3 rapid freeze-thaw cycles using liquid nitrogen for the freezing stage. Homogenization was next performed for 10 cycles as follows: ultrasonication – vortex – break. In the end, slurries were centrifuged (16000 g, 10 min) and the supernatants collected. The remaining residues were subjected once again to homogenization and centrifugation and their supernatants were combined with those from first pass extractions. Extracts were stored at -80°C until analysis.

2.5 NMR spectroscopy

Fecal extracts were thawed at room temperature and 225 µl transferred to a 5 mm NMR tube. The same volume of 99% D_2O containing 0.002% TSP [15] was added. Unidimensional standard ^{1}H NMR spectra of fecal extracts were obtained at 298 K on a Bruker Avance III spectrometer operating at 500.13 MHz for proton, using a noesy 1D pulse sequence (Bruker library) with 100 ms mixing time, a 3 µs t1 delay, and water suppression during relaxation delay and mixing time. 256 transients were acquired into 32 k complex data points, with 500.13 MHz spectral width, 4 s relaxation delay and 2.34 s acquisition time. Each free-induction-decay was multiplied by a 0.3 Hz exponential line-broadening function prior to Fourier transformation. Spectra were manually phased and baseline corrected. Chemical shifts were referenced internally to TSP at δ=0.0 ppm. Peak assignments were carried out with basis on literature [16-18] spectral databases (mainly the Bruker Biorefcode database and the human metabolome database (HMDB) [19].

Multivariate analysis was applied to the full resolution ^{1}H NMR spectra of fecal extracts, after exclusion of the water (4.60-5.05 ppm) region. Spectra were aligned using a recursive segment-wise peak alignment [20] and normalized through probabilistic quotient normalization (PQN) [21], to account for sample concentration differences. Principal component analysis (PCA) and partial least squares discriminant analysis (PLS-DA) were performed after unit variance scaling (SIMCA-P 11.5, Umetrics, Sweden). The PLS-DA loading weights were obtained by multiplying each variable by its standard deviation and were colored according to each variable importance to the projection (VIP). In addition, the relevant peaks were selected and integrated (Amix 3.9.14, BrukerBioSpin, Rheinstetten, Germany), normalized and variations assessed using the non-parametric t-test (Wilcoxon test). Effect sizes were computed for all relevant resonances ($p<0.05$) [22]. Statistical tests, boxplots and loadings plots were carried out using R-statistical software (version 3.2.0, R Project) and MATLAB (version 8.3.0, MathWorks Inc.).

 doi:10.20944/preprints201801.0210.v1

2.6 DNA extraction

Frozen fecal samples were immediately weighed. Upon thawing, 300 µl of sterile phosphate buffer (PBS 1x) was added and the mixture was submitted to ultrasonication for 20 min. To the fecal slurry were added 270 µl of lysis buffer (MagNa Pure Bacteria Lysis Buffer, Roche, Basel, Switzerland) and 30 µl of proteinase K (Qiagen, Netherlands). This mix was incubated at 65°C for 10 min., vortexed and incubated for 10 min at 95°C. Samples were filtered in a filter tube (Becton DiKinson Biosciences) to remove the debris and the filtrate was centrifuged (9000 RPM, 15 min, 4°C) and the supernatant collected. DNA was extracted using a kit (MagNa Pure Nucleic Acid Isolation Kit I, Roche, Basel, Switzerland) and performed on a MagNa Pure Compact Instrument (Roche, Basel, Switzerland). Fecal DNA samples were then stored at -80°C.

2.7 Quantitative PCR

Real-time quantitative PCR (qPCR) was used to quantify populations of total bacteria, enterobacteria and lactobacilli. Specific reactions for each different type of bacteria were carried on with specific different primers [23]. For total bacteria, the following 16S rRNA primer [24] was used: F (forward) 5′ AACGCGAAGAACCTTAC 3′, R (reverse) 5′ CGGTGTGTACAAGACCC 3′. For enterobacteria: F (forward) 5′ ATGGCTGTCGTCAGCTCGT 3′, R (reverse) 5′ CCTACTTCTTTTGCAACCCACTC 3′. For lactobacilli: F (forward) 5′ GCAGCAGTAGGGAATCTTCCA 3′, R (reverse) 5′ GCATTYCACCGCTACACAT 3′. The specificity of the primers was tested by sequencing of the amplicon resulting from the PCR reaction of one sample of fecal DNA. Standard curves were established prior to sample analysis using plated cultures of *Escherichia Coli* (*E. coli)* and *lactobacillus fermentum*. DNA was extracted, PCR products were purified, and concentrations were measured by spectrophotometry, at 260 nm (Eppendorf Biophotometer ®). DNA from *E.coli* was used for the total bacteria standard curve. For *E. coli*, 10^4-10^{10} gene copies were used to establish the linearity of standard curves while for *Lactobacillus*, 10^5-10^{10} copies were used. Real time PCR reactions for bacteria quantification were carried out on a LightCycler ® (Roche, Basel, Switzerland). PCR reactions were prepared on a total volume of 20 µl containing 2 µl of LightCycler FastStart DNA MasterPLUS SYBR Green I (Roche, Basel, Switzerland), 0.3 µM of each specific primer and 2 µl of DNA sample, diluted 1/100. To exclude carryover contamination a negative control was included in each PCR experiment.

3. Results

3.1. Weight gain and glucose tolerance

Mice fed with either glucose or fructose carbohydrate diets had overall similar weight gains to those fed with standard chow over the 10-week period, as shown in Figure 1a. At weeks 4 and 6 of feeding schedule, the group of fructose-fed mice had significantly less weight gain compared to either glucose- or normal chow-fed mice, but by week 10, growth rates from the three groups had converged. Glucose tolerance, as assessed by the area under the curve (AUC) of plasma glucose levels from 0-120 minutes following an oral glucose load showed no significant differences between the different diets, nor were there any significant longitudinal changes in this parameter (**Figure 1**b-e). However, by the end of the study, the group fed with fructose carbohydrate showed a tendency towards faster recovery from the glucose load and presented significantly lower values of circulating glucose at 120 min post-load (Figure 1e).

Preprints (www.preprints.org) | NOT PEER-REVIEWED | Posted: 23 January 2018 doi:10.20944/preprints201801.0210.v1

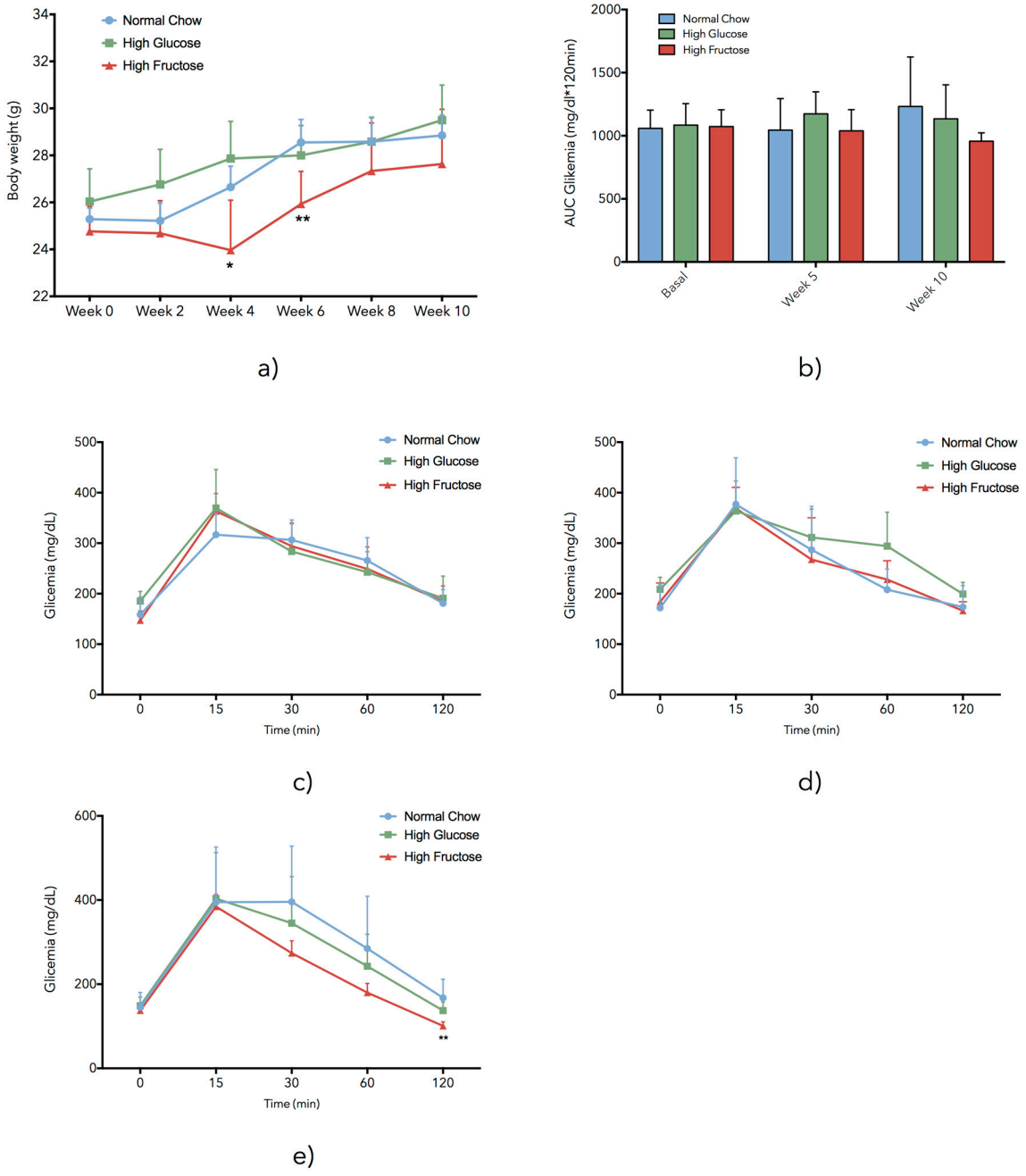

Figure 1- OGTT Profiles - Body weight alteration along time and oral glucose tolerance tests (OGTT) performed at 3 time points (Week 0, Week 5, Week 10): a) Body weight curves monitored each two weeks of the three different diets; b) Area under the curve (AUC) of the different obtained profiles for OGTT tests on week 0, week 5 and week 10; c), d) and e) OGTT profiles for the three different diets groups performed at week 0, week 5 and week 10, respectively. Label shows statically significant data: * $p < 0,05$; ** $p < 0,01$; $n = 6$

3.2 Fecal Metabolite Profiles

A typical ^{1}H NMR spectrum of a fecal extract of a mouse before intervention (Figure 2) shows the predominance of branched-chain amino acids (BCCA) and other amino acids (threonine, alanine, lysine, aspartate, taurine, tyrosine and phenylalanine), several organic acids (butyrate, propionate, lactate, acetate, pyruvate, succinate, fumarate, 4-hydroxyphenylacetate (4-HPA) and formate), trimethylamine (TMA), methanol, uracil and xylose. Table S1 lists the full set of identified spin

Preprints (www.preprints.org) | NOT PEER-REVIEWED | Posted: 23 January 2018 doi:10.20944/preprints201801.0210.v1

systems. PCA scores of all ^{1}H NMR spectra for the three groups of animals (Figure 3a) shows that normal (blue) and high-glucose (green) diets have similar effects on fecal extracts metabolic profile, with slightly higher dispersion for the latter (Figure 3a,c).

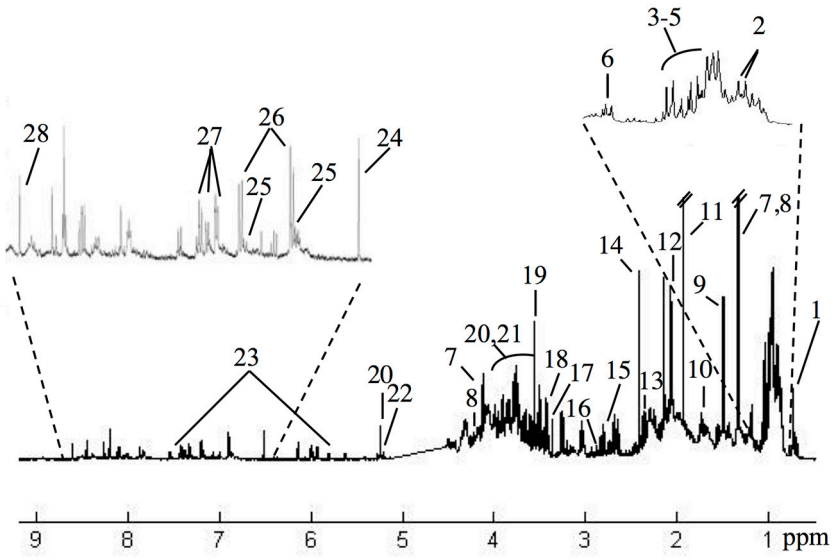

Figure 2 – Typical ^{1}H NMR spectrum of a rat fecal extract at week 0 - Main assignments shown: 1, bile acids (tentative assignment), 2, butyrate; 3, leucine; 4, isoleucine; 5, valine; 6, propionate; 7, lactate; 8, threonine, 9, alanine; 10, lysine; 11, acetate; 12, N-acetylglycoproteins; 13, pyruvate; 14, succinate; 15, aspartate; 16, TMA (trimethylamine); 17, methanol; 18, taurine; 19, glycine; 20, xylose; 21, α-glucose; 22, β-glucose 23, uracil; 24, fumarate; 25, 4-HPA (4-hydroxyphenylacetate); 26, tyrosine; 27, phenylalanine; 28, formate.

Conversely, the high-fructose diet induces significant changes in about half of the samples considered and suggests two different directions in PCA space (Figure 3a, b), although apparently not following a clear uniform trend in terms of time progression. Pairwise PLS-DA scores (Figure 4, left) confirm the separation of high-fructose diet from both normal and high-glucose diets (Figure 4a, c) and indicate a small separation between animals on high-glucose and normal chow diets (Figure 4b). The reasons for these separations were sought through inspection of PLS-DA loading weights (Figure 4, right), peak integration and univariate analysis. Table 1 lists all relevant metabolite changes separating animal classes based on their diet, also represented in boxplot form (Figures S1 to S3), which however do not consider the animal time-course evolution of each animal.

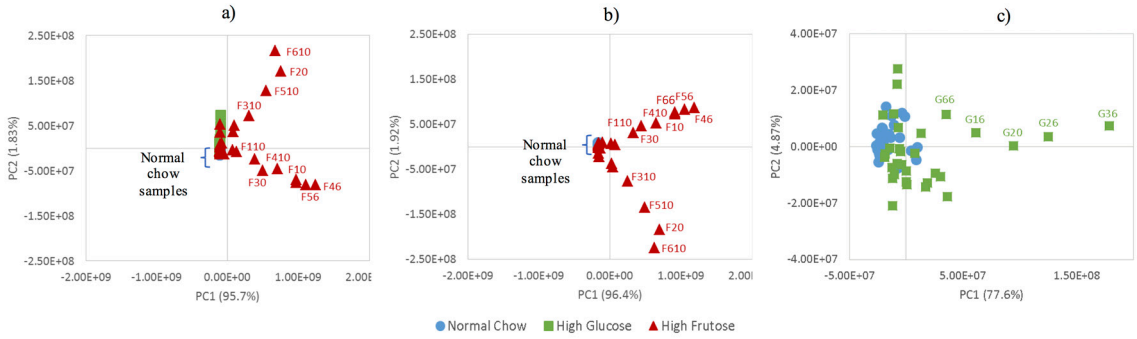

Figure 3 - PCA scores scatter plots using the ^{1}H NMR spectra of fecal extracts - for a) all three diets, b) normal chow and high-fructose diets and c) normal chow and high-glucose diets (note the lower range in PC axis in c), in order to clarify the relatively smaller distinction between the two diets). Outlier G12 was removed from dataset. Sample labeling indicate F/G for high-fructose or glucose diets, followed by number of mouse and number of week e.g. G12: high-glucose-fed mouse 1 at week 2.

Preprints (www.preprints.org) | NOT PEER-REVIEWED | Posted: 23 January 2018 doi:10.20944/preprints201801.0210.v1

It becomes apparent that a set of 12 metabolites seem to be particularly important in differentiating the animals subjected to fructose-chow, from the other two diets, namely: butyrate, fructose, glucose, glutamate, lactate, phenylalanine, propionate, succinate, tyrosine, uracil, xylose and unassigned singlet at δ 8.73. The average time trajectories of these metabolites characterize fructose-chow compared to glucose- and normal-chow (Figure 5). Butyrate is at a persistently lower level (except for week 8) and a similar, but not as marked, tendency is seen for glutamate levels. Propionate levels remain close to normal chow, again except at week 8. Fructose, succinate, phe, tyr and xylose all exhibit relatively higher levels. As seen by the magnitude of the error bars, these metabolite levels showed high inter-animal variability – with the sole exception of fructose. Lactate overlaps with threonine and lactate/thr levels increase at week 10, albeit with high variability. The unassigned singlet at δ 8.03 exhibits consistently low levels in fructose-chow compared to normal-chow and glucose-chow groups so that, despite remaining unidentified, this resonance seems to be part of the high-fructose metabolic signature.

In addition, the interesting bidirectional behavior of the animals fed with high-fructose diet (Figures 3 and 4) was further explored through PLS-DA of the deviant high-fructose samples (Figure S4), revealing that such separation is mainly due to the different degrees of fructose malabsorption, mostly at weeks 6 and 10, although high inter-animal variability is also noted.

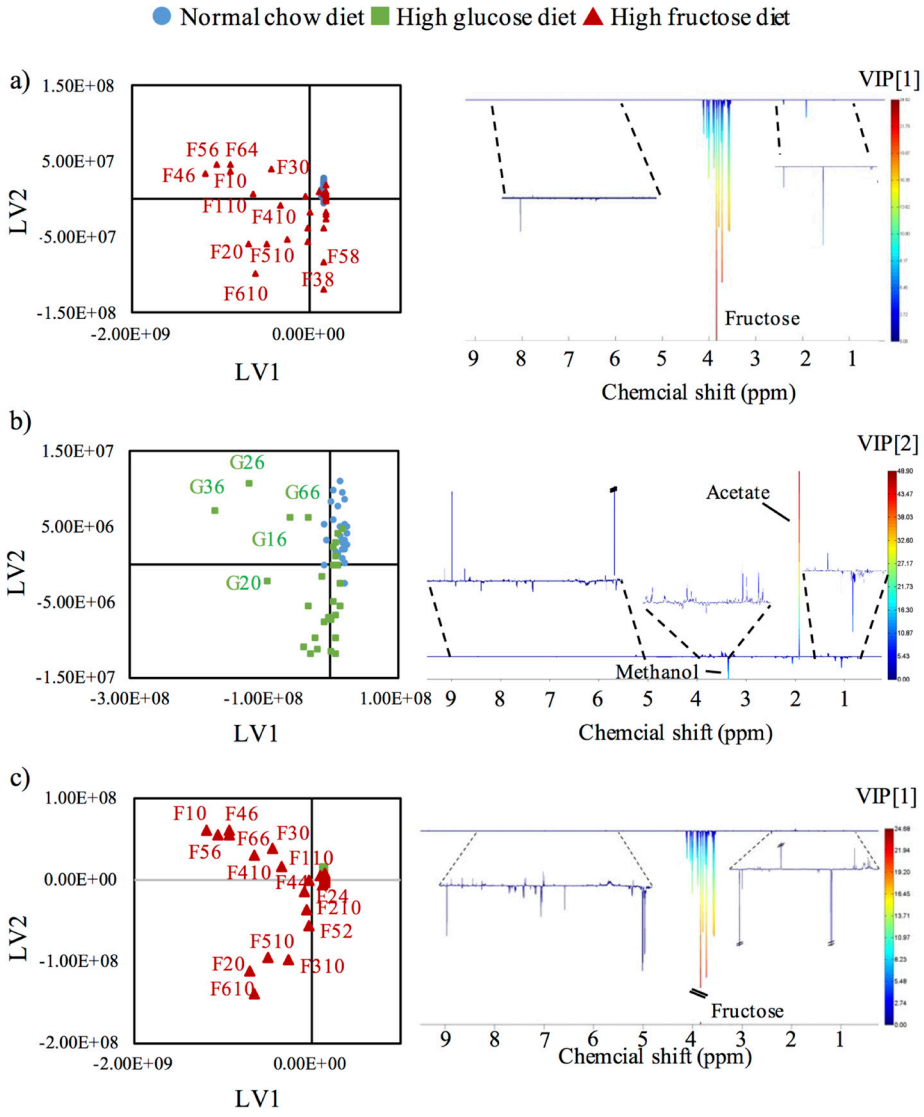

Figure 4 - PLS-DA scores (left) and loadings weights (right) - for animals fed with a) high-fructose *vs* normal chow, b) high-glucose *vs* normal chow, c) high-fructose *vs* high-glucose diets (outlier G12 was removed from dataset).

 doi:10.20944/preprints201801.0210.v1

247

248 **Table 1 -** Statistically relevant (p-value < 0.05) metabolite changes separating animal classes based on
249 their diet. The chemical shifts shown correspond to the integrated peaks (Table S1 lists the full set of
250 spin systems). N, normal chow; F, high-fructose diet; G, high-glucose diet. Values correspond to
251 changes in the first named group, compared to the second named group e.g. aspartate is decreased in
252 G, compared to N. ES: effect size. Ui: unassigned resonances. s: singlet, dd: doublet of doublets, t:
253 triplet, m: multiplet.

254

255

		G vs N		F vs N		F vs G	
Metabolite	**δ/ppm (multiplicity)**	**ES**	**p-value**	**ES**	**p-value**	**ES**	**p-value**
Acetate	1.92 (s)	0.96±0.53	1.4E-6	1.12±0.54	1.2E-7	-	-
Aspartate	2.82 (dd)	-1.38±0.56	6.6E-8	-1.38±0.56	4.9E-7	-	-
Butyrate	0.90 (t)	-	-	-0.86±0.52	2.9E-3	-1.06±0.53	1.6E-4
Formate	8.46 (s)	0.69±0.52	6.6E-5	1.36±0.55	5. 3E-8	-	-
Fructose	4.04 (m)	-	-	1.07±0.53	7.2E-8	1.07±0.53	1.0E-6
Glucose	5.23 (d)	-	-	-	-	0.77±0.51	9.7E-3
Glutamate	2.15 (m)	-	-	-0.79±0.52	2.1E-3	-	-
Methanol	3.36 (s)	0.58±0.51	1.1E-4	0.80±0.52	1.1E-5	-	-
Lactate/ threonine	1.33 (d)	-	-	-	-	0.61±0.51	8.2E-3
Phenylalanine	7.34 (m), 7.38 (m)	-	-	0.80±0.52	3.7E-3	0.55±0.50	1.3E-2
Propionate	2.18 (q)	0.92±0.53	7.6E-4	-	-	-0.55±0.50	1.1E-2
Pyruvate	2.38 (s)	0.69±0.52	3.7E-2	0.74±0.52	1.2E-3	-	-
Succinate	2.41 (s)	-	-	1.40±0.56	6.6E-9	0.99±0.52	6.6E-6
Taurine	3.43 (t)	0.75±0.52	6.1E-5	1.70±0.58	4.2E-9	1.02±0.53	9.4E-5
Tyrosine	7.20 (d)	-	-	0.66±0.51	2.7E-2	0.69±0.51	5.8E-3
Uracil	7.58 (d)	-	-	-0.56±0.50	3.7E-3	-	-
Xylose	5.21 (d)	-	-	1.53±0.57	5.7E-10	0.78±0.51	1.1E-3
U1	8.03 (s)	-	-	-	-	-0.72±0.51	6.3E-3
U2	8.62 (s)	-1.21±0.55	4.7E-6	-1.11±0.54	5.6E-5	-	-

256

Preprints (www.preprints.org) | NOT PEER-REVIEWED | Posted: 23 January 2018 doi:10.20944/preprints201801.0210.v1

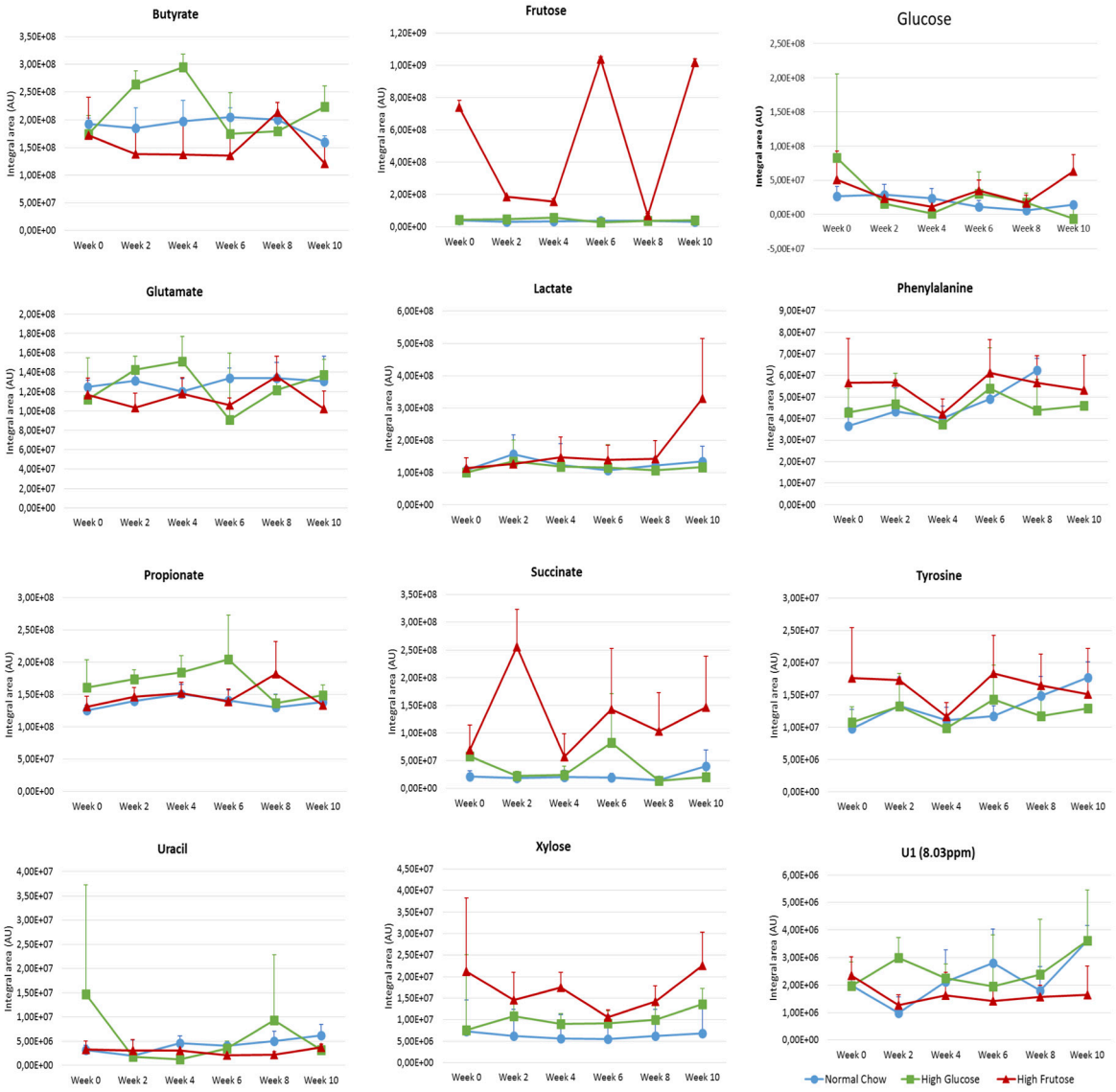

Figure 5 - Time-course variations for the main metabolites - distinguishing animals fed with high-fructose diet from those fed with normal chow or high-glucose diet. These 12 metabolites have been selected from the data in Table 1. Normal chow: blue line, high-glucose: green line, high-fructose, red line.

3.3 Fecal Microbial Profiles

The intestinal microbiota has a significant role in dietary carbohydrate metabolism, in particular the fermentative breakdown of complex carbohydrates into simple absorbable metabolites such as short chain fatty acids (SCFA) [25]. Recent studies suggest that increased consumption of simple over complex carbohydrates promotes intestinal dysbiosis and wider metabolic disruption. Since this particular dysbiosis is thought to be associated with a shift in bacterial populations from gram-positive to gram-negative species [26], we compared the intervals of normal-chow, glucose-chow and fructose-chow feeding on the abundances of *Enterobacteria* and *Lactobacillus*, representative of gram-positive and gram-negative bacterial groups, respectively. The total abundances of *Enterobacteria* and *Lactobacillus* showed a high amount of variability between individuals of the same diet, as shown in the supplemental data (Table S2). To get a measure of shifts between gram positive and gram-negative populations, ratios of *Enterobacteria* to total and *Lactobacillus* to total were calculated. These data are summarized by the heatmaps in Figure 6a, b. While the proportion of *Enterobacteria* generally increased over the 10-week period for all three diets,

Preprints (www.preprints.org) | NOT PEER-REVIEWED | Posted: 23 January 2018 doi:10.20944/preprints201801.0210.v1

the rate of increase was slower for glucose- and fructose-chow compared to standard chow (Figure 6a). The proportion of *Lactobacillus* showed a general decrease in mice fed normal chow or glucose-chow over the 10-week interval. However, for mice fed with fructose-chow, the proportion of *Lactobacillus* increased over the same period (Figure 6b). Given that the *Lactobacillus* genre encompasses fructophilic bacteria, and that our NMR data showed a carry-over of dietary fructose into feces, these results could reflect an intestinal substrate profile that favors the growth of *Lactobacillus* over other species under conditions of high fructose feeding.

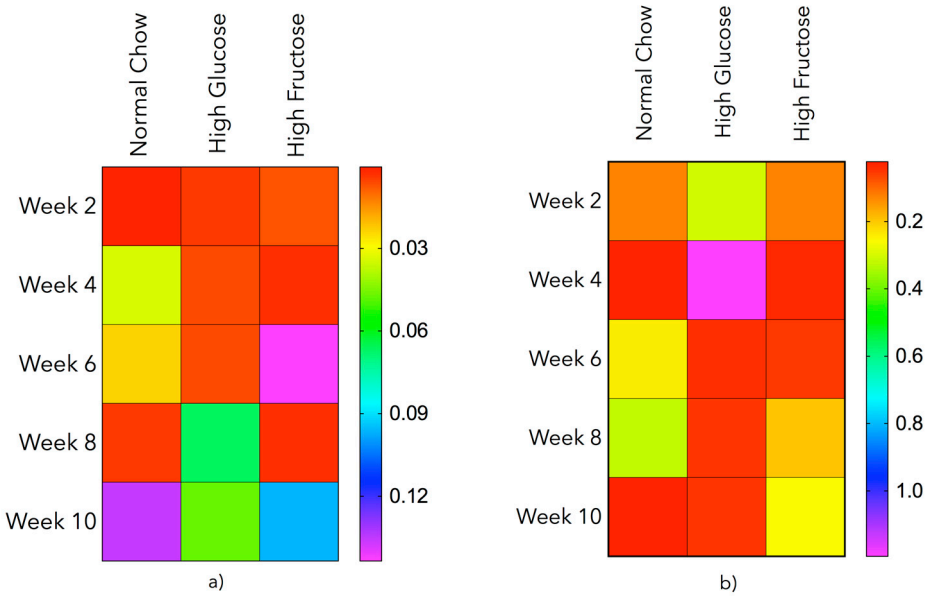

Figure 6 - Heatmaps of the variation of: a) *Enterobacteria* and b) *Lactobacillus* portion content over total bacteria along time every two weeks for 10 weeks.

4. Discussion

4.1 Replacement of normal chow carbohydrate with pure glucose or fructose for 10 weeks did not result in increased body weight or glucose intolerance

Our study showed that for C57BL/6 mice, substitution of normal chow carbohydrate constituents[1] with pure glucose over a period of 10 weeks did not significantly alter overall weight gain, and were in fact gaining significantly less weight up until the sixth week of the study. Mice that received fructose-chow had noticeably slower weight gain compared to both glucose-chow and normal-chow groups. These observations match those of Mellor et al., who found that either weaned or adult mice fed for 6 weeks with fructose-chow[2] showed 11% and 18% less weight gain, respectively, compared to controls fed with standard chow [27]. We also did not see any significant differences in glucose tolerance between the three groups. In the study of Nunes et al. where mice were fed for 8 weeks with glucose- and fructose-chow formulations identical to those used in our study, no differences in glucose tolerance and insulin sensitivity were observed, while weight gain was significantly less for the mice fed with fructose-chow [28]. Hence, for our study, the fecal metabolite and microbiota distributions observed for the three diets were not related to differences in body weight gain and/or glucose tolerance status.

[1] This consists of a mixture of cornstarch, maltodextrin and sucrose in proportions of 4.0:1.3:1.0.

[2] The diet composition was essentially the same as that used in our study.

 doi:10.20944/preprints201801.0210.v1

4.2 Incomplete intestinal fructose absorption

In mice provided with fructose-chow, there were significant amounts of unabsorbed fructose in the feces indicating insufficient intestinal capacity for its absorption. There were no significant levels of hexose in the feces of either glucose-chow or normal-chow fed mice. Intestinal fructose absorption is largely mediated by the constitutive GLUT-5 transporter [29], whose expression is upregulated by high-fructose feeding [30]. Despite this, it appears that at least in humans, the intestinal capacity for fructose uptake is overwhelmed by high fructose intake, resulting in malabsorption and discomfort from microbial fructose fermentation [31,32]. While defective fructose absorption has been previously documented in GLUT5-knockout mice [29], to our knowledge our study is the first to report incomplete fructose absorption in wild-type mice. Given that fructose absorption is facilitated by the presence of dietary glucose [28], the absence of glucose in the high-fructose chow may have potentiated its incomplete absorption by mice that were fed on this diet.

4.3 Effects of fructose- and glucose-chow on fecal extract metabolite profiles

The intestinal microbiota is associated with a complex array of intra- and extracellular metabolites. Some of these are end-products of nutrient breakdown that are cleared into the surrounding medium, for example SCFA and lactate, while others represent intracellular metabolic pathway intermediates. Since feces contain a very high density of bacteria, the fraction of the total metabolite recovery contributed by intracellular sources is likely to be considerably high, given that intracellular concentrations of certain metabolites such as glutamate and taurine can reach millimolar levels. Moreover, metabolic products of one bacterium species may be utilized for energy and/or converted to new metabolites by another species. Thus, the effects of different diets on the profile of metabolites that are likely to be predominantly intracellular, which includes taurine, glutamate and aromatic amino acids, involve complex metabolic interactions both within and between different bacterial species. We will focus on those metabolites that are considered to have a significant influence on host metabolic health.

Alterations in SCFA production – namely acetate, propionate and butyrate – via microbial fermentation are recognised as key links between intestinal microbiota activity and risks for metabolic diseases such as Type 2 diabetes and NAFLD [26,33]. Butyrate is a preferred oxidative substrate for enterocyte energy generation, and it also shows tumour suppression and anti-inflammatory effects [34,35]. Our results indicate that mice fed with fructose-chow had lower levels of fecal butyrate compared to those fed glucose- or normal chow. If this was a limiting factor in enterocyte energy generation, it could compromise energy-intensive enterocyte functions such as tight-junction maintenance thereby increasing intestinal permeability and leakage of proinflammatory endotoxin into portal vein blood - which provokes hepatic inflammation [5,6]. Such a mechanism might contribute to the so-called “second hit”; a cellular insult that when superimposed on high lipid levels transforms benign NAFLD into more severe forms such as non-alcoholic steatohepatitis (NASH). Other animal studies have demonstrated a link between dietary fructose supplementation, increased intestinal permeability, and augmented NAFLD severity. In a study of C57BL/6 mice fed with either normal chow or a Western-style diet high in fat and sugar, the addition of fructose to the drinking water increased endotoxin translocation for both diets [36]. In normal-chow-fed mice that were supplemented with 30% fructose in the drinking water, elevated hepatic lipid and plasma transaminase levels were associated with impaired intestinal barrier function and increased concentrations of portal plasma endotoxin [37]. Since these studies did not examine the effects of fructose supplementation on fecal SCFA levels, a direct link between the detrimental effects of high fructose feeding on intestinal integrity and a decreased abundance of fecal butyrate remains to be established. Interestingly, certain *Lactobacilli* counteract the inhibition of enterocyte butyrate uptake by enteropathogenic *E. coli* [38]. Thus, the increased abundance of *Lactobacilli* over *Enterobacteria* that we observed in fructose-chow fed mice over glucose- and normal-chow fed animals could mitigate the lower abundance of butyrate.

Acetate, which accounts for the large majority (60-80%) of intestinal SCFA production, was elevated in mice fed with both glucose- and fructose-chow compared to normal-chow fed animals,

 doi:10.20944/preprints201801.0210.v1

while propionate levels were not different between fructose-chow and normal-chow fed animals but were significantly higher in the glucose-chow fed group. Whether increased intestinal acetate production is beneficial or detrimental remains unclear. On the one hand, it is an agonist of the intestinal GPR43/FFAR2 receptor, that among other things promotes intestinal secretion of incretins such as GLP-1 thereby contributing to better postprandial glycemic control [39]. On the other hand, in a cross-sectional study of lean and obese youths, elevated plasma acetate levels (as well as butyrate and propionate) and enhanced fermentation of fructose by fecal microbe cultures were found to be associated with increased body mass index, adiposity and *de novo* lipogenesis rates [40]. Fecal levels of propionate, the only gluconeogenic SCFA of the three and accounting for 10-15% of SCFA production, were similar between fructose- and normal-chow fed mice but were significantly elevated in glucose-chow fed mice. As for acetate, the effects of altered intestinal propionate levels on metabolic dysfunctions associated with obesity and ectopic lipid accumulation are also unclear. Increased levels of circulating propionate has been associated with obesity and steatosis [40], while other reports claim that increased intestinal propionate levels hasten the postprandial satiety response thereby protecting against obesity [41].

The elevated levels of fecal aromatic amino acids in mice fed fructose-chow compared to either glucose- or normal-chow fed mice may have also important implications on intestinal integrity and immune status. Both tyr and phe can be metabolized by bacteria to aryl propionates via the dehydration of phenyllactic acid, mediated by phenyllactate dehydratase (PLD) [42]. Tryptophan is also degraded by this pathway to form 3-indole-propionate, a potent antioxidant that also preserves intestinal barrier function. The higher levels of tyrosine and phenylalanine observed during fructose feeding may indicate a reduced PLD aptitude, which would also result in less 3-indole propionate production from tryptophan and therefore less protection of intestinal barrier function. The higher dietary amounts of phenylalanine and tyrosine (1.07% and 0.74%, respectively), over tryptophan (0.27%) could explain their higher visibility in the ^{1}H NMR spectrum.

4.5 Variability in microbial and metabolite profiles

Our study revealed substantial variability in both fecal metabolite and microbial profiles between different animals fed with the same diet as well as for individual animals across the 10-week feeding interval. Such variability has been described in previous rodent studies [43]. In a study of repeated fecal sampling of humans, the intra-individual coefficient of variation was over 40% [44] Our results highlight the importance of multiple feces sampling during a feeding trial or interval to obtain representative levels of fecal metabolites and microbial populations.

5. Conclusions

In Western societies, increased intake of refined sugar, consisting of roughly equimolar amounts of glucose and fructose, is implicated in the surge of NAFLD and Type 2 Diabetes incidences. While glucose and fructose are isocaloric, they are metabolized quite differently by the tissues and organs of the body. Our study also indicates that intake of these sugars also results in different profiles of intestinal microbiota and their associated metabolites. The intestinal metabolite profile associated with fructose feeding seems to have more potential for inducing host metabolic disturbances compared to that of glucose, mainly through compromising intestinal barrier integrity. When taken in high amounts, intestinal fructose absorption is not quantitative hence its availability as a substrate for microbial metabolism is increased. It remains to be determined whether this characteristic explains the differences in intestinal microbiota and metabolite profiles between fructose and glucose.

Supplementary Materials: The following are available online at www.mdpi.com/link, Figure S1, S2, S3: Boxplots of all statistically relevant (p-value < 0.05) metabolite changes, Figure S4: PLS-DA scores of the two subgroups of high-fructose fed animals Table S1: List of metabolites found in the ^{1}H NMR spectra (500 MHz) of fecal extracts, Table S2: Intra and Intervariability between animals.

Acknowledgments: This project was developed within the scope of the project CICECO-Aveiro Institute of Materials, POCI-01-0145-FEDER-007679 (FCT Ref. UID /CTM /50011/2013), financed by national funds through the FCT/MEC and when appropriate co-financed by FEDER under the PT2020 Partnership Agreement. We also acknowledge the Portuguese National NMR Network (RNRMN), supported by FCT funds. Structural funding for the Center for Neuroscience and Cell Biology is supported in part by FEDER – European Regional Development Fund, within the PT2020 Partnership Agreement, and the COMPETE 2020 Programme within the project UID/BIA/04004/2013. This work was also funded through a Portuguese Foundation for Science and Technology (FCT) Investigator-initated grant PTDC-SAU-MET-111398-2009. DD acknowledges FCT fellowship grant SFRH/BD/119509/2016 and JCPS FCT fellowship grant SFRH/BD/90259/2012.

Author Contributions: JCPS, MM, CN, TG, JGJ and AMG conceived and designed the experiments; JCPS, MM and FOM performed the experiments; JCPS, MM, FOM, TC, JP, DD, ASB, JGJ and AMG analyzed the data; CN, TG, JGJ and AMG contributed reagents/materials/analysis tools; JCPS, JGJ and AMG wrote the paper.

Conflicts of Interest: The authors declare no conflict of interest.

References

1. Zimmet, P.; Shaw, J. Diabetes rising incidence of diabetes mellitus in youth in the USA. *Nature Reviews Endocrinology* **2017**, *13*, 379-U316.
2. Younossi, Z.M.; Blissett, D.; Blissett, R.; Henry, L.; Stepanova, M.; Younossi, Y.; Racila, A.; Hunt, S.; Beckerman, R. The economic and clinical burden of nonalcoholic fatty liver disease in the united states and europe. *Hepatology* **2016**, *64*, 1577-1586.
3. Jaacks, L.M.; Siegel, K.R.; Gujral, U.P.; Narayan, K.M.V. Type 2 diabetes: A 21st century epidemic. *Best Practice & Research Clinical Endocrinology & Metabolism* **2016**, *30*, 331-343.
4. Tappy, L.; Le, K.A. Metabolic effects of fructose and the worldwide increase in obesity. *Physiological Reviews* **2010**, *90*, 23-46.
5. Delzenne, N.M.; Cani, P.D. Gut microbiota and the pathogenesis of insulin resistance. *Current Diabetes Reports* **2011**, *11*, 154-159.
6. Cani, P.D.; Bibiloni, R.; Knauf, C.; Neyrinck, A.M.; Delzenne, N.M.; Burcelin, R. Changes in gut microbiota control metabolic endotoxemia-induced inflammation in high-fat diet-induced obesity and diabetes in mice. *Diabetes* **2008**, *57*, 1470-1481.
7. Cani, P.D.; Amar, J.; Iglesias, M.A.; Poggi, M.; Knauf, C.; Bastelica, D.; Neyrinck, A.M.; Fava, F.; Tuohy, K.M.; Chabo, C., *et al.* Metabolic endotoxemia initiates obesity and insulin resistance. *Diabetes* **2007**, *56*, 1761-1772.
8. David, L.A.; Maurice, C.F.; Carmody, R.N.; Gootenberg, D.B.; Button, J.E.; Wolfe, B.E.; Ling, A.V.; Devlin, A.S.; Varma, Y.; Fischbach, M.A., *et al.* Diet rapidly and reproducibly alters the human gut microbiome. *Nature* **2014**, *505*, 559-+.
9. Heinritz, S.N.; Weiss, E.; Eklund, M.; Aumiller, T.; Heyer, C.M.E.; Messner, S.; Rings, A.; Louis, S.; Bischoff, S.C.; Mosenthin, R. Impact of a high-fat or high-fiber diet on intestinal microbiota and metabolic markers in a pig model. *Nutrients* **2016**, *8*.
10. Kumari, M.; Kozyrskyj, A.L. Gut microbial metabolism defines host metabolism: An emerging perspective in obesity and allergic inflammation. *Obesity Reviews* **2017**, *18*, 18-31.
11. Francini, F.; Castro, M.C.; Schinella, G.; Garcia, M.E.; Maiztegui, B.; Raschia, M.A.; Gagliardino, J.J.; Massa, M.L. Changes induced by a fructose-rich diet on hepatic metabolism and the antioxidant system. *Life Sciences* **2010**, *86*, 965-971.
12. Dekker, M.J.; Su, Q.; Baker, C.; Rutledge, A.C.; Adeli, K. Fructose: A highly lipogenic nutrient implicated in insulin resistance, hepatic steatosis, and the metabolic syndrome. *Am J Physiol Endocrinol Metab* **2010**, *299*, E685-694.
13. Kawasaki, T.; Igarashi, K.; Koeda, T.; Sugimoto, K.; Nakagawa, K.; Hayashi, S.; Yamaji, R.; Inui, H.; Fukusato, T.; Yamanouchi, T. Rats fed fructose-enriched diets have characteristics of nonalcoholic hepatic steatosis. *Journal of Nutrition* **2009**, *139*, 2067-2071.
14. Rutledge, A.C.; Adeli, K. Fructose and the metabolic syndrome: Pathophysiology and molecular mechanisms. *Nutrition Reviews* **2007**, *65*, S13-S23.
15. Zhao, Y.; Wu, J.; Li, J.V.; Zhou, N.Y.; Tang, H.; Wang, Y. Gut microbiota composition modifies fecal metabolic profiles in mice. *J Proteome Res* **2013**, *12*, 2987-2999.

16. Yang, Y.; Wang, L.; Wang, S.; Huang, R.; Zheng, L.; Liang, S.; Zhang, L.; Xu, J. An integrated metabonomic approach to studying metabolic profiles in rat models with insulin resistance induced by high fructose. *Mol Biosyst* **2014**, *10*, 1803-1811.
17. Hong, Y.S.; Ahn, Y.T.; Park, J.C.; Lee, J.H.; Lee, H.; Huh, C.S.; Kim, D.H.; Ryu, D.H.; Hwang, G.S. 1h nmr-based metabonomic assessment of probiotic effects in a colitis mouse model. *Arch Pharm Res* **2010**, *33*, 1091-1101.
18. Zhang, C.; Li, S.; Yang, L.; Huang, P.; Li, W.; Wang, S.; Zhao, G.; Zhang, M.; Pang, X.; Yan, Z., *et al.* Structural modulation of gut microbiota in life-long calorie-restricted mice. *Nat Commun* **2013**, *4*, 2163.
19. Wishart, D.S.; Knox, C.; Guo, A.C.; Eisner, R.; Young, N.; Gautam, B.; Hau, D.D.; Psychogios, N.; Dong, E.; Bouatra, S., *et al.* Hmdb: A knowledgebase for the human metabolome. *Nucleic Acids Res* **2009**, *37*, D603-610.
20. Veselkov, K.A.; Lindon, J.C.; Ebbels, T.M.; Crockford, D.; Volynkin, V.V.; Holmes, E.; Davies, D.B.; Nicholson, J.K. Recursive segment-wise peak alignment of biological (1)h nmr spectra for improved metabolic biomarker recovery. *Anal Chem* **2009**, *81*, 56-66.
21. Dieterle, F.; Ross, A.; Schlotterbeck, G.; Senn, H. Probabilistic quotient normalization as robust method to account for dilution of complex biological mixtures. Application in 1h nmr metabonomics. *Anal Chem* **2006**, *78*, 4281-4290.
22. Berben, L.; Sereika, S.M.; Engberg, S. Effect size estimation: Methods and examples. *Int J Nurs Stud* **2012**, *49*, 1039-1047.
23. Castillo, M.; Martin-Orue, S.M.; Manzanilla, E.G.; Badiola, I.; Martin, M.; Gasa, J. Quantification of total bacteria, enterobacteria and lactobacilli populations in pig digesta by real-time pcr. *Vet Microbiol* **2006**, *114*, 165-170.
24. van Minnen, L.P.; Timmerman, H.M.; Lutgendorff, F.; Verheem, A.; Harmsen, W.; Konstantinov, S.R.; Smidt, H.; Visser, M.R.; Rijkers, G.T.; Gooszen, H.G., *et al.* Modification of intestinal flora with multispecies probiotics reduces bacterial translocation and improves clinical course in a rat model of acute pancreatitis. *Surgery* **2007**, *141*, 470-480.
25. Koh, A.; De Vadder, F.; Kovatcheva-Datchary, P.; Backhed, F. From dietary fiber to host physiology: Short-chain fatty acids as key bacterial metabolites. *Cell* **2016**, *165*, 1332-1345.
26. Arora, T.; Backhed, F. The gut microbiota and metabolic disease: Current understanding and future perspectives. *J Intern Med* **2016**, *280*, 339-349.
27. Mellor, K.; Ritchie, R.H.; Meredith, G.; Woodman, O.L.; Morris, M.J.; Delbridge, L.M. High-fructose diet elevates myocardial superoxide generation in mice in the absence of cardiac hypertrophy. *Nutrition* **2010**, *26*, 842-848.
28. Nunes, P.M.; Wright, A.J.; Veltien, A.; van Asten, J.J.; Tack, C.J.; Jones, J.G.; Heerschap, A. Dietary lipids do not contribute to the higher hepatic triglyceride levels of fructose- compared to glucose-fed mice. *FASEB J* **2014**, *28*, 1988-1997.
29. Barone, S.; Fussell, S.L.; Singh, A.K.; Lucas, F.; Xu, J.; Kim, C.; Wu, X.; Yu, Y.; Amlal, H.; Seidler, U., *et al.* Slc2a5 (glut5) is essential for the absorption of fructose in the intestine and generation of fructose-induced hypertension. *J Biol Chem* **2009**, *284*, 5056-5066.
30. Patel, C.; Douard, V.; Yu, S.; Tharabenjasin, P.; Gao, N.; Ferraris, R.P. Fructose-induced increases in expression of intestinal fructolytic and gluconeogenic genes are regulated by glut5 and khk. *Am J Physiol Regul Integr Comp Physiol* **2015**, *309*, R499-509.
31. Latulippe, M.E.; Skoog, S.M. Fructose malabsorption and intolerance: Effects of fructose with and without simultaneous glucose ingestion. *Crit Rev Food Sci Nutr* **2011**, *51*, 583-592.
32. Jones, H.F.; Butler, R.N.; Brooks, D.A. Intestinal fructose transport and malabsorption in humans. *Am J Physiol Gastrointest Liver Physiol* **2011**, *300*, G202-206.
33. Sonnenburg, J.L.; Backhed, F. Diet-microbiota interactions as moderators of human metabolism. *Nature* **2016**, *535*, 56-64.
34. van der Beek, C.M.; Dejong, C.H.C.; Troost, F.J.; Masclee, A.A.M.; Lenaerts, K. Role of short-chain fatty acids in colonic inflammation, carcinogenesis, and mucosal protection and healing. *Nutr Rev* **2017**, *75*, 286-305.
35. Jin, U.H.; Cheng, Y.; Park, H.; Davidson, L.A.; Callaway, E.S.; Chapkin, R.S.; Jayaraman, A.; Asante, A.; Allred, C.; Weaver, E.A., *et al.* Short chain fatty acids enhance aryl hydrocarbon (ah) responsiveness in mouse colonocytes and caco-2 human colon cancer cells. *Sci Rep* **2017**, *7*, 10163.

36. Volynets, V.; Louis, S.; Pretz, D.; Lang, L.; Ostaff, M.J.; Wehkamp, J.; Bischoff, S.C. Intestinal barrier function and the gut microbiome are differentially affected in mice fed a western-style diet or drinking water supplemented with fructose. *J Nutr* **2017**, *147*, 770-780.

37. Spruss, A.; Kanuri, G.; Stahl, C.; Bischoff, S.C.; Bergheim, I. Metformin protects against the development of fructose-induced steatosis in mice: Role of the intestinal barrier function. *Lab Invest* **2012**, *92*, 1020-1032.

38. Kumar, A.; Alrefai, W.A.; Borthakur, A.; Dudeja, P.K. Lactobacillus acidophilus counteracts enteropathogenic e. Coli-induced inhibition of butyrate uptake in intestinal epithelial cells. *Am J Physiol Gastrointest Liver Physiol* **2015**, *309*, G602-607.

39. Chambers, E.S.; Morrison, D.J.; Frost, G. Control of appetite and energy intake by scfa: What are the potential underlying mechanisms? *Proc Nutr Soc* **2015**, *74*, 328-336.

40. Goffredo, M.; Mass, K.; Parks, E.J.; Wagner, D.A.; McClure, E.A.; Graf, J.; Savoye, M.; Pierpont, B.; Cline, G.; Santoro, N. Role of gut microbiota and short chain fatty acids in modulating energy harvest and fat partitioning in youth. *J Clin Endocrinol Metab* **2016**, *101*, 4367-4376.

41. Arora, T.; Sharma, R.; Frost, G. Propionate. Anti-obesity and satiety enhancing factor? *Appetite* **2011**, *56*, 511-515.

42. Dodd, D.; Spitzer, M.H.; Van Treuren, W.; Merrill, B.D.; Hryckowian, A.J.; Higginbottom, S.K.; Le, A.; Cowan, T.M.; Nolan, G.P.; Fischbach, M.A., *et al.* A gut bacterial pathway metabolizes aromatic amino acids into nine circulating metabolites. *Nature* **2017**, *551*, 648-652.

43. Franklin, C.L.; Ericsson, A.C. Microbiota and reproducibility of rodent models. *Lab Anim (NY)* **2017**, *46*, 114-122.

44. Lamichhane, S.; Sundekilde, U.K.; Blaedel, T.; Dalsgaard, T.K.; Larsen, L.H.; Dragsted, L.O.; Astrup, A.; Bertram, H.C. Optimizing sampling strategies for nmr-based metabolomics of human feces: Pooled vs. Unpooled analyses. *Anal Methods-Uk* **2017**, *9*, 4476-4480.